Electronic Supplementary Information

Oxygen vacancies promoting the electrocatalytic activity of dual-shelled $Co_3V_2O_8$ hollow sphere catalyst for efficient oxygen evolution

Long Li,[a] Xiantao Lin[a] and Qiang Hu*[a,b]

[a]Department of Chemistry, Lishui University, Lishui 323000, P. R. China.

[b]Zhejiang Zhentai Energy Technology Co. Ltd, Lishui, 323000, China.

E-mail: qihu@z-etech.cn

1 Materials characterizations

The phase formation was identified using powder X-ray diffraction (XRD) (Bruker D8, Cu-Kα). The morphologies of the catalysts were observed by field emission scanning electron microscopy (FE-SEM, HITACHI S-4800) and transmission electron microscopy (TEM, JEOL JEM-2010). The linear scanning energy-dispersive X-ray spectrometry (EDX) and EDX elemental mappings were taken on TEM. The X-ray photoelectron spectroscopy (XPS) spectra were measured on ESCALAB 250 spectrometer (Perkin-Elmer). Raman spectra were analyzed using in-Via Raman spectrometer.

2 Electrochemical measurements

The electrochemical tests were conducted on CHI 760E electrochemical workstation. The Ag/AgCl (saturated KCl solution) as used as the reference electrode, a graphite rod was served as the counter electrode, and all NiO spheres catalysts were utilized as working electrode. All electrochemical tests were performed in 1 M KOH aqueous electrolyte and the catalysts were dissolved in ethanol solution and then uniformly cast onto glassy carbon working electrode with a total loading of 0.4 mg cm^{-2}. All the linear sweep voltammetry (LSV) measurements were taken at a scan rate of 5 mV s^{-1} to obtain the polarization curves. Chronoamperometric measurements were performed at corresponding potential to deliver a current density of 10 mA cm^{-2}. The Tafel slope was calculated according to the Tafel equation $\eta = b \log (j/j_0)$ (η is the overpotential, b is the Tafel slope, j is the current density, and j_0 is the exchange current density). Potentials were referenced to a reversible hydrogen electrode (RHE) using the following equation: Potentials were referenced to a reversible hydrogen electrode (RHE) using the following equation: E (RHE) =E (Ag/AgCl) + (0.205 + 0.059pH) V. The double layer capacitance (C_{dl}) was obtained using cyclic voltammetry (CV) scanning from 1.22 to 1.28 V vs. RHE with different scan rates from 20 to 60 mV s^{-1} for OER. The electrochemical impedance spectroscopy (EIS) measurements were carried out by ranging the frequency from 100 k Hz to 0.1 Hz.

2. Supplementary figures

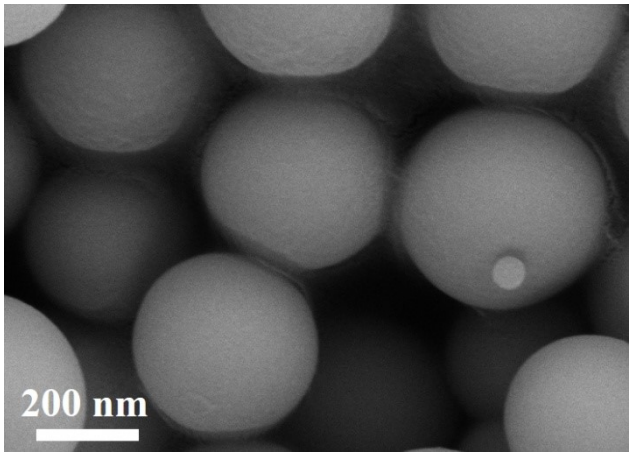

Fig. S1 SEM image of the CoV-precursor sample.

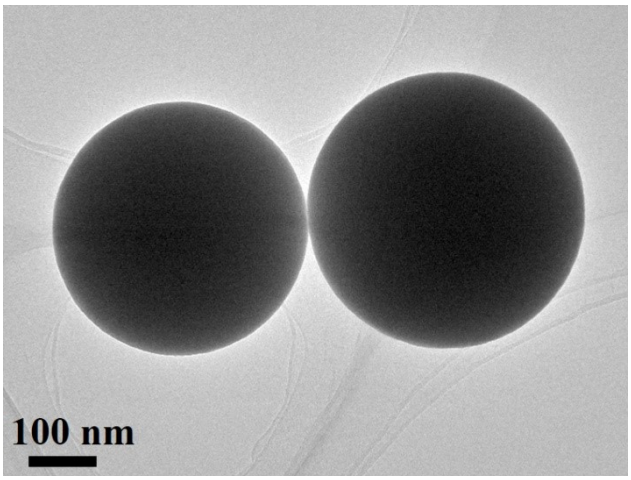

Fig. S2 TEM image of the CoV-precursor sample.

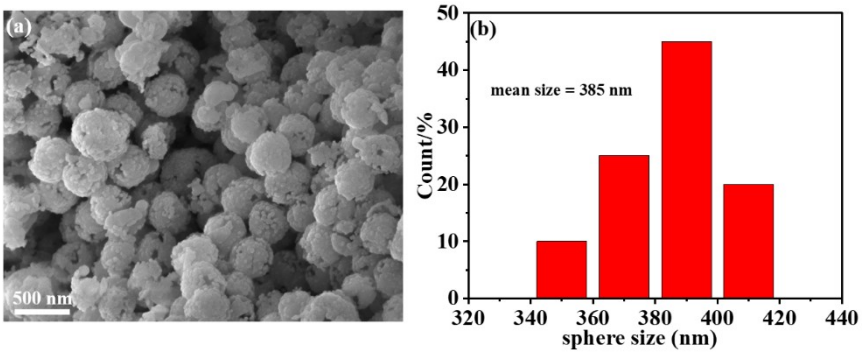

Fig. S3 (a) SEM image for $Co_3V_2O_8$-1h spheres and (b) spheres size distribution for $Co_3V_2O_8$-1h spheres.

SEM image with associated size distributions of $Co_3V_2O_8$-1h spheres are shown in Fig. S3. It is clear that the spheres are homogeneous and the average size is about 385 nm.

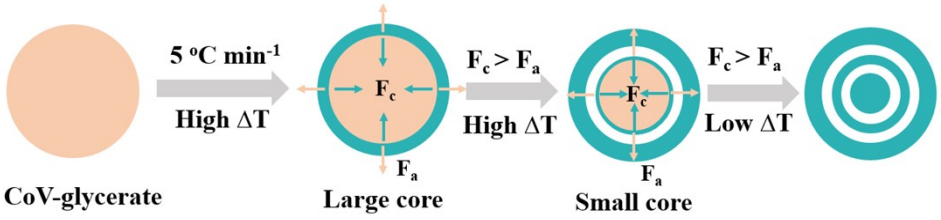

Fig. S4 Illustration of the formation process for the dual shell.

We have now presented the formation process of dual shell, as shown in Fig. S4, and CoV-glycerate is a kind of metal alkoxides, containing a large amount of organic species.[1-3] These organic species in CoV-glycerate spheres are easily released by being combusted into carbon dioxide and water during calcination, accompanied by inward shrinkage and weight loss of CoV-glycerate spheres. At the initial stage of calcination, there will be a high temperature gradient (ΔT) along the radial direction in CoV-glycerate spheres, which leads to the metal hydroxides just in the surface of CoV-glycerate spheres being dehydrated into metal oxides and then forming a rigid shell. Thereafter, there will be an interface between the outermost layer and the CoV-glycerate core in the CoV-glycerate spheres, and there will be two forces in opposing

directions acting on the interface between the shell and the CoV-glycerate core. One is the cohesive force (F_c) caused by the weight loss during calcination, leading to inward shrinkage of the CoV-glycerate core.[1] The other is the adhesive force (F_a) from the shell, which hinders the inward shrinkage of the CoV-glycerate core. When $F_c > F_a$ with a large temperature gradient, the inner core will contract inward and exfoliate from the shell resulting in the formation of the core-shell structure. And if the core-shell structure possesses large enough core, the core can generate another rigid shell on the out surface under an inhomogeneous heating, cloning the evolution process of the CoV-glycerate precursors because of the still high ΔT in its radial direction and thus generate dual shell.

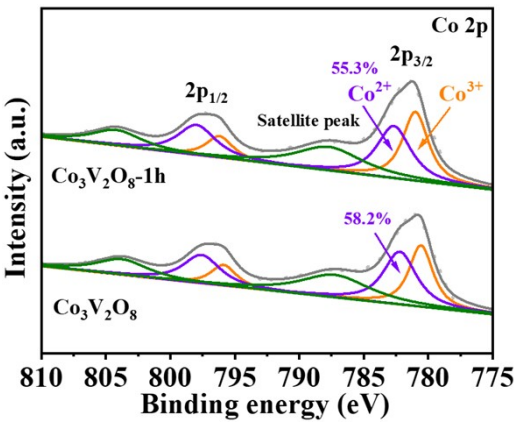

Fig. S5 Co 2p X-ray photoelectron spectra of of $Co_3V_2O_8$ and $Co_3V_2O_8$-1h spheres.

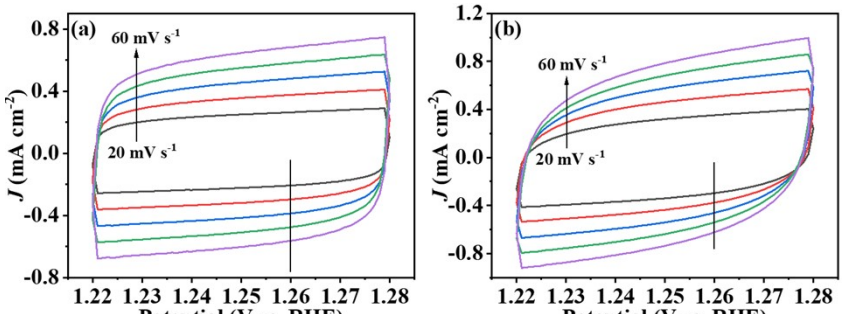

Fig. S6 CVs tested at the potential range of 1.22 –1.28 V vs. RHE with the scan rates increasing from 20 to 60 mV s^{-1} for (a) $Co_3V_2O_8$, (b) $Co_3V_2O_8$-0.5h, (c) $Co_3V_2O_8$-1h and (d) $Co_3V_2O_8$-2h spheres.

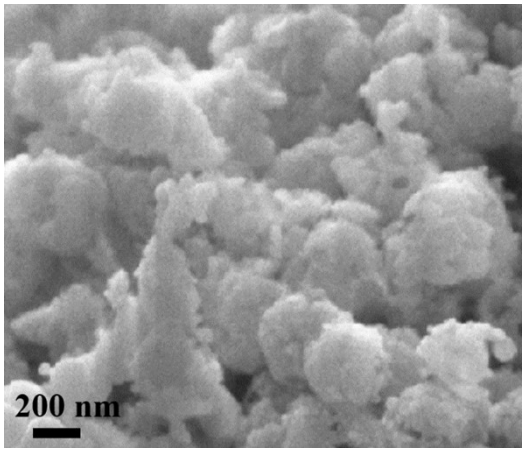

Fig. S7 SEM images of $Co_3V_2O_8$-1h spheres after 12 h chronoamperometric test.

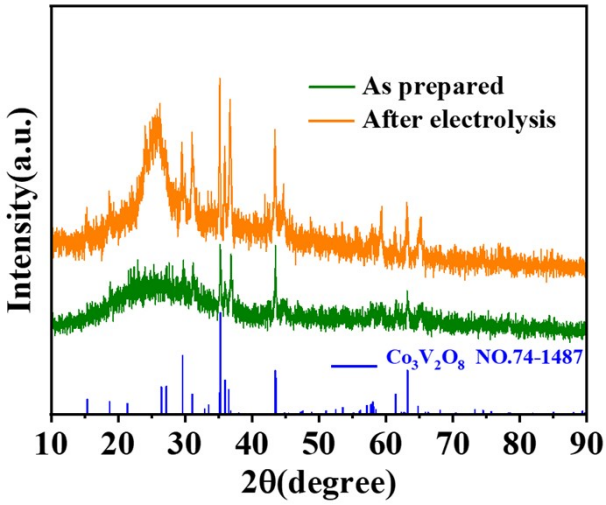

Fig. S8 XRD of Co_3V_2 [illegible] test.

We have now presented SEM and XRD after 12 h chronoamperometric test in Supporting Information, as shown in Fig. S7 and S8, respectively. In Fig. S7, the $Co_3V_2O_8$-1h spheres maintained the hollow structure after 12 h chronoamperometric test. And in Fig. S8, the unchanged number of the XRD peaks comfirms that $Co_3V_2O_8$-1h spheres preserve the crystal structure of $Co_3V_2O_8$ rather than transform to CoOOH during OER process. The stable crystal structure of $Co_3V_2O_8$ may derives from its specific cobalt local environment.[4]

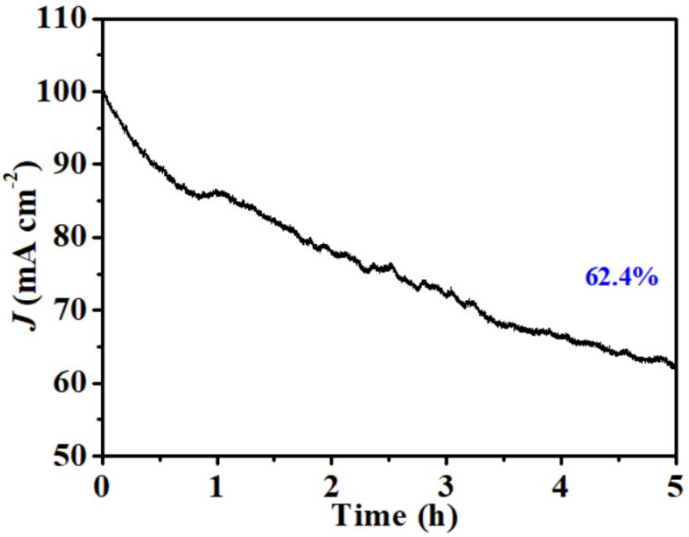

Fig. S9 Chronoamperometric response at a current density of 100 mA cm^{-2} for 5 h for $Co_3V_2O_8$-1h spheres.

The stability test at higher current density of 100 mA cm^{-2} was performed. As shown in Fig.S9, $Co_3V_2O_8$-1h spheres demonstrated huge drop in current density after 5 h of continuous operation, and the unsatisfactory performance may come from the fact that the larger current density leads to the production of a large number of bubbles, resulting in severe catalyst shedding.

References

1. L. Shen, L. Yu, X.Y. Yu, X. Zhang and X. W. Lou, *Angew. Chem. Int. Ed.*, 2015, **54**, 1868-1872.
2. D. Larcher, G. Sudant, R. Patrice and J. M. Tarascon, *Chem. Mater.*, 2003, **15**, 3543-3551.
3. J. Zhao, Y. Zou, X. Zou, T. Bai, Y. Liu, R. Gao, D. Wang and G.-D. Li, *Nanoscale*, 2014, **6**, 7255-7262.
4. H. Kim, J. Park, I. Park, K. Jin, S. E. Jerng, S. H. Kim, K. T. Nam and K. Kang, *Nat. Commun.*, 2015, **6**, 8253.